Journal of Engineering Mathematics 18 (1984) 119–132

The evolution of a two-dimensional small-amplitude voidage disturbance in a uniformly fluidized bed

D.J. NEEDHAM and J.H. MERKIN

Department of Applied Mathematical Studies, University of Leeds, Leeds LS2 9JT, UK

(Received September 13, 1983)

Summary

The evolution of a small-amplitude localized voidage disturbance through a two-dimensional fluidized bed is considered. A solution of the full initial-value problem reveals that the stability condition for the uniform state is found to be in agreement with that given by Needham and Merkin [1] for narrow beds. Further, it is shown that for a given flow rate for which the uniform state is unstable, more and more cross-channel modes become unstable with increasing bed width, in accordance with the observations of Didwania and Homsy [3]. Finally a solution is obtained for $F \ll 1$, where F is the Froude number. The resulting Fourier series is summed numerically, which enables the evolution of the initial disturbance to be followed by plotting contours of constant voidage with increasing time. This shows that in narrow beds the motion is primarily one-dimensional, confirming the supposition of [1], with cross-stream variations becoming more dominant as the bed width increases.

1. Introduction

In this paper we consider the two-dimensional evolution of a small-amplitude localized voidage disturbance through a fluidized bed. Primarily we are able to show that the uniformly fluidized state is stable only when $\bar{P}_0 \geqslant C_0^2$ where $\bar{P}_0$ is the coefficient of the interparticle collisional pressure term, $C_0 = (n+1)(1-\epsilon_0)$ is the linearized propagation speed of the zeroth cross-channel mode and ϵ_0 is the uniform voidage for the given flow rate. This result is in agreement with the stability condition for the uniform state in narrow beds (Needham and Merkin [1]). Also, when conditions are such that the uniform state is unstable, i.e. at flow rates for which $\bar{P}_0 < C_0^2$ it is shown that, as the width of the bed increases, more and more cross-channel modes, with increasing wave number become unstable. This is in agreement with the observations of El-Kaissy and Homsy [2] and Didwania and Homsy [3], who noted that with increasing flow rate, planar voidage waves develop strong cross-channel instabilities in the form of transverse voidage oscillations which eventually wrap around each other, forming small bubble-like clusters of high voidage.

For conditions when the uniform state is stable, i.e. when $\bar{P}_0 \geqslant C_0^2$, we are able to write the full solution of the initial value problem as a Fourier series. This series is then examined in detail in the case when $F \ll 1$ (where F is the Froude number); a condition which is satisfied in most gas fluidized beds. This solution is summed numerically for given localized initial conditions for varying $\sigma = d/h$, where d is the bed width and h is the vertical length scale of the initial disturbance. This shows that for $\sigma \ll 1$ the motion is essentially one-dimensional, consisting of a horizontal band of high voidage propagating vertically upwards through the bed with speed C_0, leaving behind the rest of the initial disturbance which remains almost stationary. With σ of $O(1)$ a horizontal band of high voidage still propagates upwards through the bed, but this is now followed by a slower-moving "mushroom" shaped region of high voidage which is itself surrounded at the sides and below by regions of low voidage. For $\sigma \gg 1$, the propagating band is seen to disappear, with all the motion being concentrated into the propagation of a "mushroom"-shaped region of high voidage upwards through the bed.

When conditions are such that the uniform state is unstable, it is further suggested that the above results may be interpreted as the initiation of slugging in beds with $\sigma \ll 1$, confirming with [1], while in larger width beds ($\sigma \gg 1$) this may represent the initial development of the "bubbling" regime.

2. Equations of motion

The equations of motion for fluidized beds in which $\rho_f/\rho_s \ll 1$ (where ρ_f and ρ_s are the fluid and particle densities respectively) are, after neglecting terms of $O(\rho_f/\rho_s)$

$$\frac{\partial E}{\partial t} + \operatorname{div}(E\boldsymbol{u}) = 0, \tag{1}$$

$$-\frac{\partial E}{\partial t} + \operatorname{div}(1 - E)\boldsymbol{v} = 0, \tag{2}$$

$$\rho_s(1 - E)\left[\frac{\partial \boldsymbol{v}}{\partial t} + (\boldsymbol{v} \cdot \nabla)\boldsymbol{v}\right] = \beta(E)(\boldsymbol{u} - \boldsymbol{v}) - (1 - E)\rho_s g\boldsymbol{i} - \nabla P_s + \mu_s \nabla^2 \boldsymbol{v}, \tag{3}$$

$$\nabla p = -\beta(E)(\boldsymbol{u} - \boldsymbol{v}). \tag{4}$$

Here $\boldsymbol{u}$ is the fluid phase velocity, $\boldsymbol{v}$ the particle phase velocity, E the voidage, p the fluid phase pressure, μ_s the particle phase viscosity and $\boldsymbol{i}$ a unit vector directed vertically upwards. $\beta(E)$ is the drag coefficient per unit bed volume, and $P_s(E)$ the particle phase pressure, both of which depend on E. The equations are closed once this functional dependence is proposed. Following [1] we take,

$$\beta(E) = \frac{D_0(1 - E)}{V_p E^n}, \tag{5}$$

$$P_s(E) = P_0(1 - E), \tag{6}$$

where D_0 is the Stokes drag on a single particle, V_p is the volume of a single particle and $n \simeq 3.0$ for a gas fluidized bed. P_0 is a constant, having the dimensions of pressure and is of the order of 10 dynes cm^{-2} to be consistent with values used by Anderson and Jackson [4]. The functional forms for β and P_s given by (5) and (6) are suggested by correlations of experimentally determined results, with the nature of the solution not being critically dependent on the exact forms taken for β and P_s provided only they have the same qualitative forms as (5) and (6).

Detailed derivations of the equations of motion are given by Anderson and Jackson [5] and Murray [6], in which the physical significance of each term is discussed in some detail.

3. Boundary conditions

In this paper we consider the two-dimensional flow bounded by two vertical plane walls. We introduce a Cartesian coordinate system (x, y) where x measures distance vertically upwards and y distance horizontally. The boundary walls are then fixed at $y = 0$ and $y = d$. The coordinate system is illustrated in Fig. 1.

For an "inviscid" flow, in which $\mu_s = 0$, the appropriate boundary conditions on the side walls are zero normal fluid and particle velocities. It can then be immediately deduced from Eqn. (3) that the appropriate condition on E is

$$\frac{\partial E}{\partial y} = 0 \quad \text{on} \quad y = 0 \quad \text{and} \quad y = d. \tag{7}$$

On taking into account the particle phase viscosity, we require a further boundary condition on the side walls. This is obtained as a no-slip condition on the particles at the walls [4]. Therefore, on writing $\boldsymbol{u} = (u_1, u_2)$ and $\boldsymbol{v} = (v_1, v_2)$ the boundary conditions on the fluid and particle velocities are

$$u_2 = 0 \quad \text{on} \quad y = 0 \quad \text{and} \quad y = d, \tag{8}$$

$$v_1 = v_2 = 0 \quad \text{on} \quad y = 0 \quad \text{and} \quad y = d. \tag{9}$$

The boundary conditions (7)–(9), together with the condition that, as $|x| \to \infty$, the flow is undisturbed, are now sufficient to determine the solution completely when suitable initial conditions are imposed.

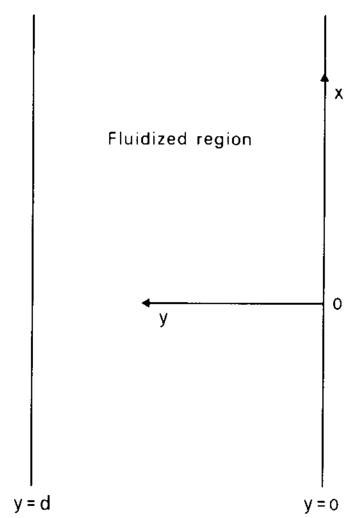

Figure 1. The coordinate system.

4. The initial-value problem

The simplest solution of Eqns. (1)–(3) satisfying the boundary conditions (7)–(9) is that in which the bed is uniformly fluidized, where

$$\boldsymbol{u} = U_0 \boldsymbol{i}, \qquad \boldsymbol{v} = 0 \qquad \text{and} \qquad E = \epsilon_0 \tag{10}$$

with $U_0 = [(1-\epsilon_0)\rho_s g]/\beta_0$ and $\beta_0 = \beta(\epsilon_0)$. This uniform state is used to introduce the following dimensionless quantities,

$$\boldsymbol{u} = U_0 \boldsymbol{u}', \qquad \boldsymbol{v} = U_0 \boldsymbol{v}', \qquad x = hx', \qquad y = hy',$$

$$t = \frac{h}{U_0} t', \qquad P_s = \rho_s U_0^2 P_s' \qquad \text{and} \qquad \beta = \frac{\rho_s U_0}{h} \beta'$$

where h is the length scale of the imposed voidage disturbance in the vertical direction. On substituting into Eqns. (1)–(3) and on dropping primes for convenience we obtain the following set of dimensionless equations

$$\frac{\partial E}{\partial t} + \operatorname{div}(E\boldsymbol{u}) = 0, \tag{11}$$

$$-\frac{\partial E}{\partial t} + \operatorname{div}((1-E)\boldsymbol{v}) = 0, \tag{12}$$

$$(1-E)\left(\frac{\partial \boldsymbol{v}}{\partial t} + \boldsymbol{v}\cdot\nabla\boldsymbol{v}\right) = \beta(E)(\boldsymbol{u}-\boldsymbol{v}) - \frac{(1-E)}{F}\boldsymbol{i} - \nabla P_s - \frac{1}{R}\nabla^2\boldsymbol{v}, \tag{13}$$

where now

$$\beta(E) = \frac{(1-E)}{F}\left(\frac{\epsilon_0}{E}\right)^n, \qquad P_s(E) = \bar{P}_0(1-E) \qquad \text{with} \quad \bar{P}_0 = \frac{P_0}{\rho_s U_0^2},$$

$F = U_0^2/(gh)$ is the Froude number and $R = (\rho_s U_0 h)/\mu_s$ is the particle-phase Reynolds number.

In terms of the dimensionless quantities the uniform state is $\boldsymbol{u} = \boldsymbol{i}$, $\boldsymbol{v} = 0$ and $E = \epsilon_0$.

We now examine the evolution of a small-amplitude voidage disturbance imposed on this uniform state at $t = 0$. The initial conditions are taken to be

$$E(x, y, 0) = \epsilon_0 + \alpha g(x, y), \tag{14}$$

$$\boldsymbol{v}(x, y, 0) = 0, \tag{15}$$

$$\boldsymbol{u}(x, y, 0) = \boldsymbol{i} + \alpha\boldsymbol{\omega}(x, y) \tag{16}$$

where $|\alpha| \ll 1$ and $\boldsymbol{\omega} = (\omega_1, \omega_2)$. To be consistent with Eqns. (11) and (12) we must also have

$$\operatorname{div}[(\epsilon_0 + \alpha g)(\boldsymbol{i} + \alpha\boldsymbol{\omega})] = 0. \tag{17}$$

A solution of Eqns. (11)–(13) is sought in the form

$$E = \epsilon_0 + \alpha \bar{E}, \qquad \boldsymbol{v} = \alpha \bar{\boldsymbol{v}}, \qquad \boldsymbol{u} = \boldsymbol{u} + \alpha \bar{\boldsymbol{u}}. \tag{18}$$

Expressions (18) are now substituted into Eqns. (11)–(13) and, on retaining terms of $O(\alpha)$ only, the following linearised equations for the perturbed quantities $\bar{E}$, $\bar{\boldsymbol{v}}$ and $\bar{\boldsymbol{u}}$ are obtained,

$$\frac{\partial \bar{E}}{\partial t} + \frac{\partial \bar{E}}{\partial x} + \epsilon_0 \operatorname{div} \bar{\boldsymbol{u}} = 0, \tag{19}$$

$$-\frac{\partial \bar{E}}{\partial t} + (1 - \epsilon_0) \operatorname{div} \bar{\boldsymbol{v}} = 0, \tag{20}$$

$$(1 - \epsilon_0) \frac{\partial \bar{\boldsymbol{v}}}{\partial t} = \frac{(1 - \epsilon_0)}{F} (\bar{\boldsymbol{u}} - \bar{\boldsymbol{v}}) + \left(\beta_0' + \frac{1}{F} \right) \bar{E} \boldsymbol{i} + \bar{P}_0 \nabla \bar{E} + R^{-1} \nabla^2 \bar{\boldsymbol{v}} \tag{21}$$

where $\beta_0' = (\mathrm{d}\beta/\mathrm{d}E)\epsilon_0$. The boundary conditions (7) and (9) become

$$\frac{\partial \bar{E}}{\partial y} = 0 \qquad \text{on} \quad y = 0 \qquad \text{and} \quad y = \sigma, \tag{22}$$

$$\bar{u}_2 = \bar{v}_1 = \bar{v}_2 = 0 \qquad \text{on} \quad y = 0 \qquad \text{and} \quad y = \sigma, \tag{23}$$

where $\sigma = d/h$, while the initial conditions (14)–(16) become

$$\bar{E}(x, y, 0) = g(x, y), \tag{24}$$

$$\bar{\boldsymbol{v}}(x, y, 0) = 0, \tag{25}$$

$$\bar{\boldsymbol{u}}(x, y, 0) = \boldsymbol{\omega}(x, y). \tag{26}$$

Condition (17) also reduces to

$$\frac{\partial \omega_1}{\partial x} + \frac{\partial \omega_2}{\partial y} = \frac{1}{\epsilon_0} \frac{\partial g}{\partial x}. \tag{27}$$

Taking the divergence of Eqn. (21) and using Eqns. (19) and (20) to eliminate div $\bar{\boldsymbol{u}}$ and div $\bar{\boldsymbol{v}}$ we obtain a single equation in $\bar{E}$, namely

$$F \frac{\partial^2 \bar{E}}{\partial t^2} = -A \frac{\partial \bar{E}}{\partial x} - B \frac{\partial \bar{E}}{\partial t} + F \bar{P}_0 \nabla^2 \bar{E} + \frac{F}{R(1 - \epsilon_0)} \frac{\partial}{\partial t} (\nabla^2 \bar{E}) \tag{28}$$

where $A = (n + 1)(1 - \epsilon_0)/\epsilon_0$ and $B = 1/\epsilon_0$. Equation (28) is to be solved subject to boundary condition (22) together with initial condition (24). Equation (28) is second order in t, we therefore require a further initial condition. This is provided via Eqn. (20) as

$$\frac{\partial \bar{E}}{\partial t} = 0 \qquad \text{at} \quad t = 0. \tag{29}$$

We look for a solution of Eqn. (28), separable in y, of the form

$$\bar{E}(x, y, t) = \bar{\psi}(x, t)\bar{\phi}(y). \tag{30}$$

Substituting (30) for $\bar{E}$ into Eqn. (28) gives, after re-arrangement,

$$\frac{F\dfrac{\partial^2\bar{\psi}}{\partial t^2} + A\dfrac{\partial\bar{\psi}}{\partial x} + B\dfrac{\partial\bar{\psi}}{\partial t} - F\bar{P}_0\dfrac{\partial^2\bar{\psi}}{\partial x^2} - \dfrac{F}{R(1-\epsilon_0)}\dfrac{\partial^3\bar{\psi}}{\partial x^2\partial t}}{\bar{\psi} + \dfrac{1}{R(1-\epsilon_0)}\dfrac{\partial\bar{\psi}}{\partial t}} = \frac{F\bar{P}_0}{\bar{\phi}}\frac{\mathrm{d}^2\bar{\phi}}{\mathrm{d}y^2} = -\lambda^2$$

where λ is a real constant. For $\bar{\phi}$ we have

$$\frac{\mathrm{d}^2\bar{\phi}}{\mathrm{d}y^2} + \frac{\lambda^2}{F\bar{P}_0}\bar{\phi} = 0 \tag{31}$$

subject to $\mathrm{d}\bar{\phi}/\mathrm{d}y = 0$ on $y = 0$ and $y = \sigma$. On solving (31) for $\bar{\phi}$ we find

$$\lambda = \frac{n\pi\sqrt{F\bar{P}_0}}{\sigma} \quad (n = 0, 1, 2, \ldots), \tag{32}$$

$$\bar{\phi}_n(y) = D_n \cos\left(\frac{n\pi y}{\sigma}\right) \quad (n = 0, 1, 2, \ldots). \tag{33}$$

where the D_n are arbitrary constants. $\bar{\psi}$ is then a solution of the equation

$$F\frac{\partial^2\bar{\psi}}{\partial t^2} + A\frac{\partial\bar{\psi}}{\partial x} + \left(B + \frac{n^2\pi^2F}{R(1-\epsilon_0)\sigma^2}\right)\frac{\partial\bar{\psi}}{\partial t}$$

$$= F\bar{P}_0\frac{\partial^2\bar{\psi}}{\partial x^2} + \frac{F}{R(1-\epsilon_0)}\frac{\partial^3\bar{\psi}}{\partial x^2\partial t} - \frac{n^2\pi^2F\bar{P}_0}{\sigma^2}\bar{\psi}. \tag{34}$$

Defining $\bar{\psi}_n(x, t)$ to be the n^{th} eigensolution of Eqn. (34), the general solution of Eqn. (28) for E may be written as a Fourier cosine series in the form

$$\bar{E}(x, y, t) = \bar{\psi}_0(x, t) + \sum_{n=1}^{\infty} \bar{\psi}_n(x, t)\cos\left(\frac{n\pi y}{\sigma}\right). \tag{35}$$

5. Stability and the solution when $\bar{P}_0 > C_0^2$

We now consider the temporal stability of the uniform state through Eqn. (34). Clearly, if any of the eigenfunctions $\bar{\psi}_n(x, t)$ grow in time, the uniform state will be unstable. We look for a solution of Eqn. (34) in the form

$$\bar{\psi}_n(x, t) = \bar{\Psi}_n(k)\,\mathrm{e}^{ikx - \omega_n t} \tag{36}$$

where k, the wave number, is real. Substitution for $\bar{\psi}_n$ from (36) into Eqn. (34) leads to a quadratic equation for ω_n in terms of k, namely

$$F\omega_n^2 - \left\{\frac{Fk^2}{R(1-\epsilon_0)} + B + \frac{n^2\pi^2 F}{R(1-\epsilon_0)\sigma^2}\right\}\omega_n + F\bar{P}_0 k^2 + Aik + \frac{n^2\pi^2 F\bar{P}_0}{\sigma^2} = 0. \quad (37)$$

A necessary and sufficient condition for the uniform state to be stable is that $\mathrm{Re}(\omega_n(k)) \geqslant 0$ for all $k > 0$ and all $n = 0, 1, 2, \ldots$ Following the method of Needham and Merkin [1], it can be shown that $\mathrm{Re}(\omega_n(k) \geqslant 0$ if and only if

$$\bar{P}_0 \geqslant \frac{A^2}{\left\{1 + \frac{n^2\pi^2}{\sigma^2 k^2}\right\}\left\{\frac{Fk^2}{R(1-\epsilon_0)} + B + \frac{n^2\pi^2 F}{R(1-\epsilon_0)\sigma^2}\right\}^2} \equiv S_n(k). \quad (38)$$

The uniform state is then stable provided

$$\bar{P}_0 \geqslant [S_n(k)]_{\max} \qquad \text{for} \quad 0 \leqslant k < \infty, \qquad n = 0, 1, 2, \ldots \quad (39)$$

An inspection of (38) reveals that (39) is satisfied if and only if

$$\bar{P}_0 \geqslant \left(\frac{A}{B}\right)^2 = C_0^2 \quad (40)$$

with $C_0 = (n+1)(1-\epsilon_0)$. Thus the uniform state is stable only when condition (40) is satisfied. It should be noted that this overall stability condition is the same as that derived in [1] for the stability of one-dimensional perturbations imposed on a uniformly fluidized bed.

Further, for a given flow rate such that $\bar{P}_0 < C_0^2$ there is an integer $N(\sigma)$ such that all cross-channel modes with $n < N$ are unstable while all cross-channel modes with $n \geqslant N + 1$ remain stable and that $N(\sigma) \to 0$ as $C_0^2 \to \bar{P}_0$ being a monotonic increasing function of C_0. Also, for C_0 fixed N is a monotonic increasing function of σ. Thus for fixed $C_0 > \sqrt{\bar{P}_0}$ an increasing number of cross-channel modes become unstable as the width of the bed is increased.

When $\bar{P}_0 > C_0^2$ the general solution of Eqn. (34) can be written in terms of Fourier integrals

$$\bar{\psi}_n(x, t) = \int_{-\infty}^{\infty} A_n(k)\, e^{ikx - \omega_n t} dk + \int_{-\infty}^{\infty} B_n(k)\, e^{ikx - \Omega_n t} dk \quad (41)$$

where $A_n(k)$ and $B_n(k)$ are arbitrary functions of k and ω_n and Ω_n are the two (complex) roots of Eqn. (37). Using (35) the complete solution may then be written as

$$\bar{E}(x, y, t) = \int_{-\infty}^{\infty} A_0(k)\, e^{ikx - \omega_n t} dk + \int_{-\infty}^{\infty} B_0(k)\, e^{ikx - \Omega_n t} dk$$
$$+ \sum_{n=1}^{\infty}\left[\int_{-\infty}^{\infty} A_n(k)\, e^{ikx - \omega_n t} dk + \int_{-\infty}^{\infty} B_n(k)\, e^{ikx - \Omega_n t} dk\right]\cos\left(\frac{n\pi y}{\sigma}\right). \quad (42)$$

The initial conditions can now be applied to (42). Applying condition (24) and using the orthogonality of the $\cos(n\pi y/\sigma)$ on $0 \leqslant y \leqslant \sigma$ we obtain

$$\int_{-\infty}^{\infty} (A_n(k) + B_n(k))\, e^{ikx} dk = \frac{2}{\sigma}\int_0^{\sigma} g(x, y) \cos\left(\frac{n\pi y}{\sigma}\right) dy, \tag{43}$$

Inverting the Fourier transforms gives

$$A_n(k) + B_n(k) = \frac{1}{\pi\sigma}\int_{-\infty}^{\infty}\left(\int_0^{\sigma} g(x, y) \cos\left(\frac{n\pi y}{\sigma}\right) dy\right) e^{-ikx} dx. \tag{44}$$

In a similar way we can apply condition (22) to obtain the equation

$$A_n(k)\omega_n(k) + B_n(k)\Omega_n(k) = 0. \tag{45}$$

Equations (44) and (45) can be solved for the A_n and B_n, resulting in

$$A_n(k) = \frac{\Omega_n}{\pi\sigma(\Omega_n - \omega_n)}\int_{-\infty}^{\infty}\left(\int_0^{\sigma} g(x, y) \cos\left(\frac{n\pi y}{\sigma}\right) dy\right) e^{-ikx} dx, \tag{46}$$

$$B_n(k) = -\frac{A_n\omega_n}{\Omega_n}. \tag{47}$$

The complete solution is then given by (42) together with (46) and (47).

6. The solution for $F \ll 1$

In many gas-fluidized beds $F \ll 1$, and with this approximation, Eqn. (34) for the eigenfunctions $\bar{\psi}_n$ reduces to

$$\frac{\partial\bar{\psi}_n}{\partial t} + \frac{A}{B + \dfrac{n^2\pi^2 F}{R(1-\epsilon_0)\sigma^2}}\frac{\partial\bar{\psi}_n}{\partial x} = 0. \tag{48}$$

Although the highest time derivative has been neglected in obtaining Eqn. (48), a consideration of a small-time solution when t is of $O(F)$, as in [1], reveals that the appropriate initial condition to be applied to the solution of Eqn. (48) is still condition (24).

The general solution of Eqn. (48) is given by

$$\psi_n(x, t) = f_n(x - C_n t) \tag{49}$$

where

$$C_n = \frac{A}{B + \dfrac{n^2\pi^2 F}{R(1-\epsilon_0)\sigma^2}} \quad (n = 0, 1, 2, \ldots). \tag{50}$$

After applying condition (24) the full solution is then given by

$$\bar{E}(x, y, t) = f_0(x - C_0 t) + \sum_{n=1}^{\infty} f_n(x - C_n t) \cos\left(\frac{n\pi y}{\sigma}\right) \tag{51}$$

where

$$f_0(\xi) = \frac{1}{\sigma}\int_0^{\sigma} g(\xi, \eta)\mathrm{d}\eta, \qquad f_n(\xi) = \frac{2}{\sigma}\int_0^{\sigma} g(\xi, \eta)\cos\frac{n\pi\eta}{\sigma}\mathrm{d}\eta. \tag{52}$$

To illustrate the nature of solution (51) we choose a particular initial voidage distribution $g(x, y)$ given by

$$g(x, y) = \frac{4y}{\sigma^2}(\sigma - y)\,\mathrm{e}^{-x^2}, \tag{53}$$

On substituting for this $g(x, y)$ into (52), we find, after integrating that

$$f_0(\xi) = \frac{2}{3}\,\mathrm{e}^{-\xi^2},$$

$$f_n(\xi) = \begin{cases} -\dfrac{16}{n^2\pi^2}\,\mathrm{e}^{-\xi^2} & (n \text{ even}), \\ 0 & (n \text{ odd}). \end{cases} \tag{54}$$

Using (54), (51) becomes

$$\bar{E}(x, y, t) = \tfrac{2}{3}\,\mathrm{e}^{-(x - C_0 t)^2} - \frac{16}{\pi^2}\sum_{n=1}^{\infty} \frac{\mathrm{e}^{-(x - C_{2n}t)^2}}{(2n)^2}\cos\left(\frac{2n\pi y}{\sigma}\right). \tag{55}$$

It can easily be shown that the series in (55) is convergent, and can be summed numerically for the voidage perturbation $\bar{E}$ for increasing time. However, before proceeding with the numerical calculation of $\bar{E}$ it is instructive to consider first the two limiting cases $\sigma \ll 1$ and $\sigma \gg 1$.

When $\sigma \ll 1$ and examination of (50) shows that $C_n \ll 1$ for $n = 1, 2, 3, \ldots$ and (55) can then be approximated by

$$\bar{E}(x, y, t) = \tfrac{2}{3}\,\mathrm{e}^{-(x - C_0 t)^2} - \tfrac{2}{3}\,\mathrm{e}^{-x^2}\left(1 - \frac{6y}{\sigma} + \frac{6y^2}{\sigma}\right) \tag{56}$$

for $0 \leqslant y \leqslant \sigma$ and $|x| < \infty$. The development as described by (56) is that of a planar voidage front propagating up the bed with speed C_0 with the remainder of the initial disturbance remaining stationary.

When $\sigma \gg 1$, (51) gives $C_n \simeq C_0$ for $n = 1, 2, 3, \ldots$ and (55) can then be approximated by

$$\bar{E}(x, y, t) = \frac{4y}{\sigma^2}(\sigma - y)\,\mathrm{e}^{-(x - C_0 t)^2} \tag{57}$$

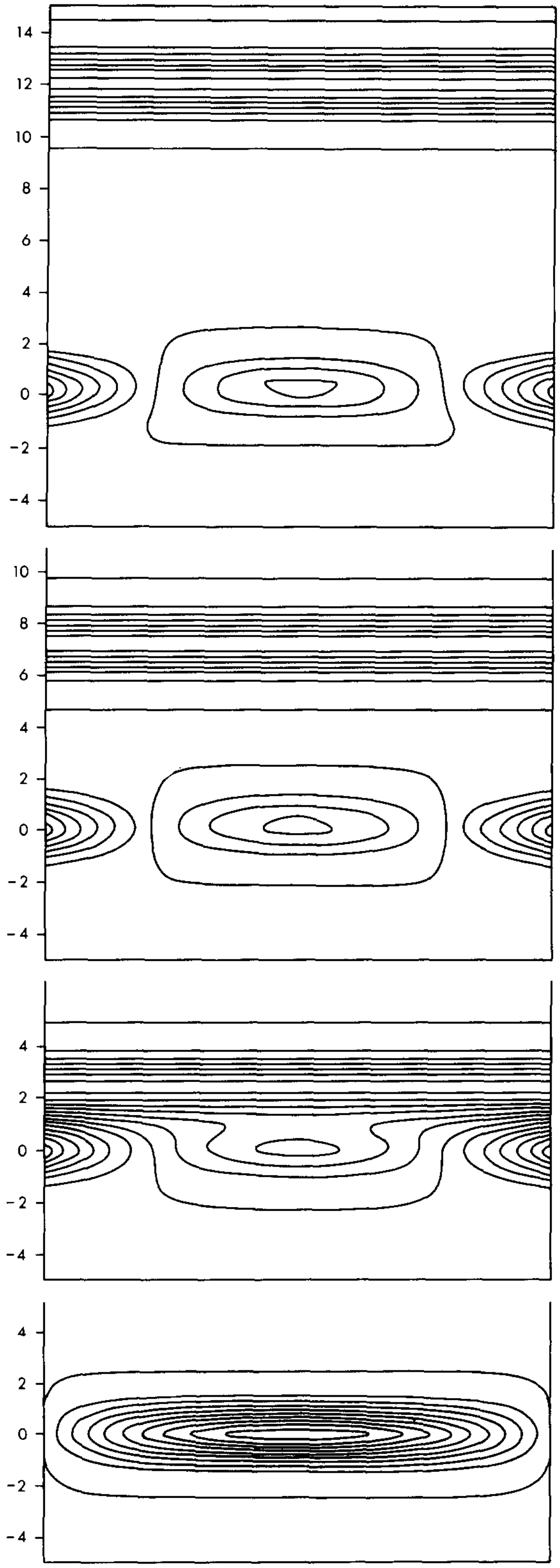

Figure 2. Contour plots of $\bar{E}$ for $\sigma = 0.25$ at $t = 0$, 1, 3 and 5.

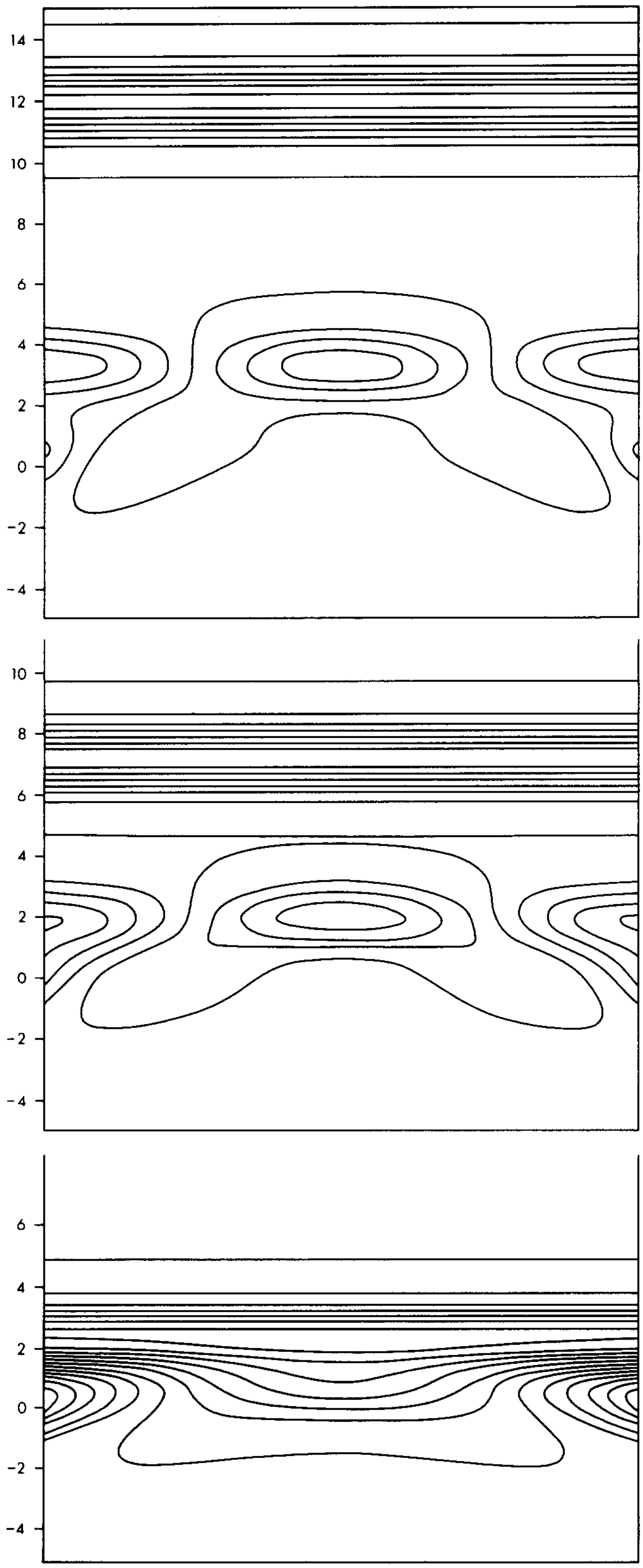

Figure 3. Contour plots of $\bar{E}$ for $\sigma = 1$ at $t = 1$, 3 and 5.

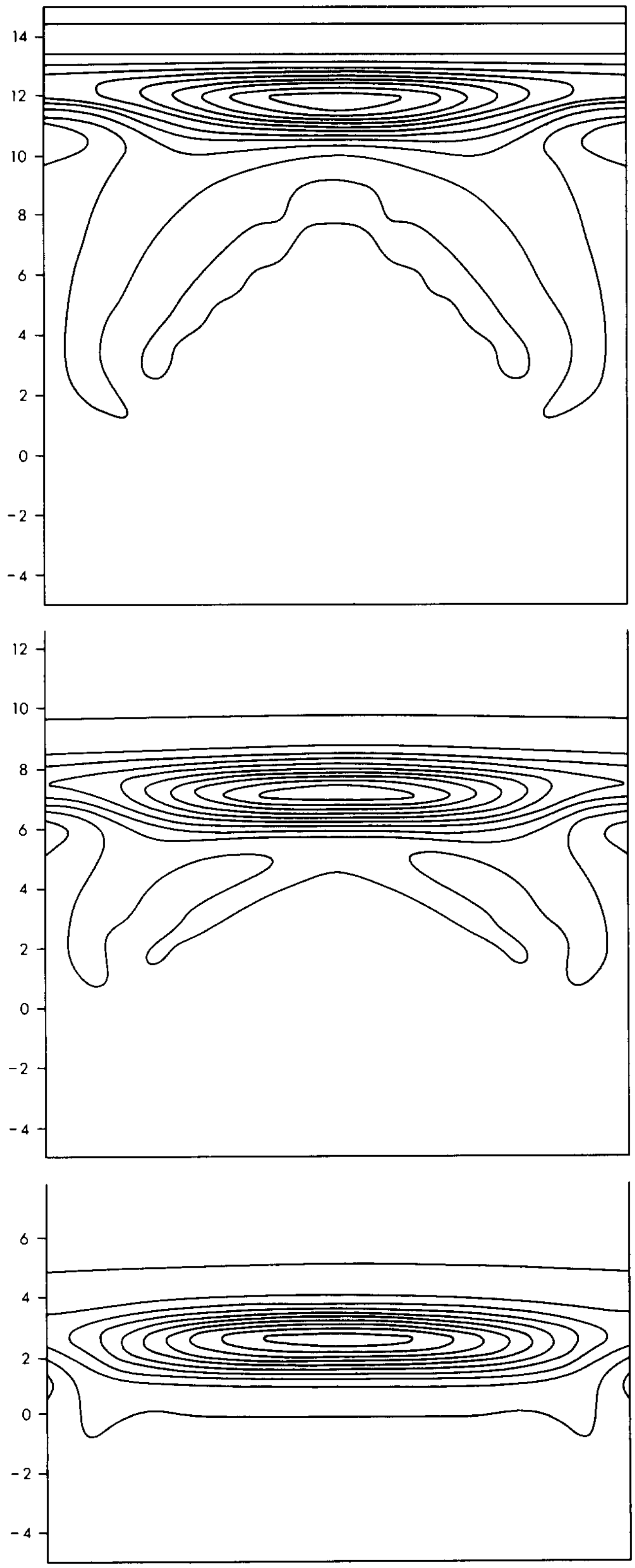

Figure 4. Contour plots of $\bar{E}$ for $\sigma = 8$ at $t = 1$, 3 and 5.

for $0 \leqslant y \leqslant \sigma$ and $|x| < \infty$. (57) shows that the initial disturbance propagates unchanged upwards through the bed with speed C_0.

We now present results obtained by summing the Fourier series (55) numerically with $\epsilon_0 = 0.4$, $R = 1.0$, $F = 0.1$, $n = 3$ and for $\sigma = 0.25$, 1.0 and 8.0. In each case we sum the series for $0 \leqslant y \leqslant \sigma$ and $-5.0 \leqslant x \leqslant 15.0$ at 20 equally spaced points in the y-direction and 40 equally spaced points in the x-direction. In all cases results are shown for times $t = 1.0$, 3.0 and 5.0. The computations were not carried out at large times as it can be shown, [1], that (55) is not uniformly valid in t, and breaks down when t is of $O(F^{-1})$, with the neglected effects of diffusion or instability and dispersion being felt on this longer time scale. Each of the above cases are shown in Figs. 2, 3 and 4 respectively, where contours of constant $\bar{E}$ are plotted in the region $0 \leqslant y \leqslant \sigma$ and $-5.0 \leqslant x \leqslant 15.0$; the contours show $\bar{E}$ between -1 and 1 in steps of 0.2. Also shown in Fig. 2 is the initial voidage perturbation as given by (53). This has the same overall shape in each of the other two cases and is not repeated.

The development of $\bar{E}$ for $\sigma = 0.25$ (Fig. 2) clearly confirms the behaviour as given by (56). It can be seen that the initial voidage perturbation breaks up into two distinct parts. There is a plane voidage front propagating upwards with a uniform speed (this is further confirmed by calculations performed at intermediate time steps not shown in the figure) with estimates of this speed giving a value very close to C_0 as given by (50), ($C_0 = 0.24$ in this case). These is also a region of voidage perturbation, two-dimensional in character, which remains behind, propagating upwards only extremely slowly. For $\sigma = 1$ (Fig. 3) the picture remains very much the same, with a plane voidage region ahead of a two-dimensional disturbance which is now propagating upward with increased speed. For $\sigma = 8$ (Fig. 4) the picture is different. Here the voidage perturbation remains two-dimensional in nature throughout and propagates upwards at a constant speed. By $t = 5$ we can see the development of a "mushroom-shaped" region of high voidage, the shape which is characteristic of "bubbles" in fluidized beds.

7. Conclusion

We have shown that the overall condition for stability of a fluidized bed, namely that $\bar{P}_0 \geqslant C_0^2$, is unaltered when two-dimensional effects are introduced. Also, when this condition is not satisfied we have shown that an increasing number of cross-channel modes become unstable as the width of the bed is increased. We have been able to solve the linear equations governing small-amplitude voidage perturbations and for the particular case of small Froude number (a situation which pertains in most gas-fluidized beds) obtaining this solutions as a Fourier cosine series which can easily be summed numerically. These results show that the nature of the flow changes as the width of the bed is increased. For narrow beds the voidage perturbations are essentially one-dimensional, confirming the validity of the one-dimensional analysis used previously by the authors [1], in discussing the full nonlinear problem. For wide beds we can detect the onset of the genuine two-dimensional nature of the flow, with the appearance of the "mushroom"-shaped regions of high voidage characteristic of a "bubbling" bed.

The work presented here needs to be taken much further before a full understanding of the nature of the transition from uniform to bubbling conditions, seen on increasing the flow rate, can be gained. The present analysis is restricted to small voidage perturbations and is valid only for values of time of $O(1)$; as shown in [1] the expansion breaks down when t is of $O(F^{-1})$, $F \ll 1$. However, given the above restrictions, the present work gives a good starting point for understanding the development of two-dimensional voidage disturbances, with, perhaps the most interesting question still remaining being in what happens to such disturbances at flow rates for which the uniform state is unstable. Can the non-linear effects re-stabilize the flow into a new quasi-steady state, as happens in the case of purely one-dimensional flow, or does some other essentially unsteady picture manifest itself? Observations of fluidized beds suggest that the former is the case with "bubbles" (regions of high voidage) propagating upwards at a steady rate (this is hinted at by the results shown in Fig. 4). This question is at present under further investigation.

Acknowledgements

This research was carried out while one of the authors (DJN) was in receipt of an SERC research studentship.

References

[1] D.J. Needham and J.H. Merkin, The propagation of a voidage disturbance in a uniformly fluidized bed, *J. Fluid Mech.* 131 (1983) 427–454.

[2] M.M. El-Kaissy and G.M. Homsy, Instability waves and the origin of bubbles in fluidized beds, part I: experiments, *Int. J. Multiphase Flow* 2 (1976) 379–395.

[3] A.K. Didwania and G.M. Homsy, Flow regimes and flow transitions in liquid fluidized beds, *Int. J. Multiphase Flow* 7 (1981) 563–580.

[4] T.B. Anderson and R. Jackson, A fluid mechanical description of fluidized beds, *Ind. Eng. Chem. Fund.* 7 (1968) 12–21.

[5] T.B. Anderson and R. Jackson, A fluid mechanical description of fluidized beds, *Ind. Eng. Chem. Fund.* 6 (1967) 527–539.

[6] J.D. Murray, On the mathematics of fluidization Part I: fundamental equations and wave propagation, *J. Fluid Mech.* 21 (1965) 465–493.